Desalination and Water Treatment
www.deswater.com
doi:10.5004/dwt.2018.22415

118 (2018) 113–119
June

A fixed-bed electrochemical reactor with nano-TiO_2 loading flat-sheet carbon membrane as anode for phenolic wastewater treatment

Hongsen Hui[a,b], Hong Wang[a,b,*], Yinghui Mo[a,c], Zhen Yin[a,c], Jianxin Li[a,b,*], Tonghua Wang[d]

[a]*State Key Laboratory of Separation Membranes and Membrane Processes/National Center for International Joint Research on Separation Membranes, Tianjin Polytechnic University, Tianjin 300387, China, Tel. +86 022 83955799; email: waho7808@163.com (H. Wang), Tel. +86 022 83955798; email: jxli@tjpu.edu.cn (J. Li), Tel. +86 022 83955798; email: huihongsen@foxmail.com (H. Hui), Tel. +86 022 83955297; email: moyinghui@sina.com (Y. Mo), Tel. +86 022 83955767; email: yinzhen163@163.com (Z. Yin)*
[b]*School of Materials Science and Engineering, Tianjin Polytechnic University, Tianjin 300387, China*
[c]*School of Environmental and Chemical Engineering, Tianjin Polytechnic University, Tianjin 300387, China*
[d]*School of Chemical Engineering, Dalian University of Technology, Dalian 116012, China, Tel. +86 0411 84986087; email: wangth@dlut.edu.cn*

Received 29 October 2017; Accepted 22 April 2018

ABSTRACT

Nano-TiO_2 loading flat-sheet microporous carbon membranes with four different thicknesses (4.9–10.3 mm) were prepared and employed as an anode to constitute fixed-bed electrochemical reactor (FBER) for phenolic wastewater treatment. Electroanalytic measurements were used to investigate the electrochemical properties of TiO_2/carbon membranes. Results showed that the TiO_2/carbon membrane with a thickness of 10.3 mm exhibited the best electrochemical performance. The peak current, effective surface area, charge transfer resistance (R_{CT}), and the diffusion coefficients obtained from TiO_2/carbon membrane with a thickness of 10.3 mm were 7.3 mA, 4.74 cm^2, 2.49 Ω, and 6.88×10^{-3} cm^2/s, respectively. Meanwhile, the thickness of carbon membrane electrode is also closely related to its hydrodynamic resistance and the permeability. Further, the removal rates of phenol and chemical oxygen demand (COD) obtained from TiO_2/carbon membrane with a thickness of 10.3 mm under the operating conditions of 10.0 mmol/L phenolic wastewater, residence time of 7.8 min, and current density of 1.0 mA/cm^2 were up to 89.3% and 97.5%, respectively. Moreover, the energy consumption of FBER was only 0.36 kWh/kg COD. FBER also demonstrated an excellent stability.

Keywords: TiO_2/flat-sheet carbon membrane; Fixed-bed electrochemical reactor (FBER); Electrochemical oxidation; Phenolic wastewater treatment; Chemical oxygen demand (COD)

1. Introduction

Phenolic compounds represent the most widespread pollutants in industrial wastewaters, with high toxicity and a strong ability to resist biological degradation, posing a serious threat to the environment [1]. Various methods have been proposed for the phenol treatment, such as extraction [2], biological treatment [3], chemical oxidation [4], and photocatalytic oxidation [5]. Despite all the efforts, these methods still face some challenges such as low efficiency and generation of toxic by-products [6]. As an alternative method in toxic organic pollutants treatment, anodic oxidation of phenolic compounds has gained the attention of researchers as its high efficiency and no additional chemical use, in many case, a complete degradation of organic pollutants into very small and noxious species. For instance, Zhu et al. [7] reported a boron-doped diamond (BDD) anode to treat phenol simulated wastewater. Results showed that BDD anode system could easily reduce the chemical oxygen demand (COD) of phenol from 633 to 145 mg/L with the energy consumption (EC) 63 kWh/kg COD. Moreover, Wei et al. [8] design

* Corresponding author.

1944-3994/1944-3986 © 2018 Desalination Publications. All rights reserved.

a pulse-BDD anode system for electrochemical oxidation of 500 mg/L phenol simulated wastewater, under the current density of 6–38 mA/cm^2, 80% of COD was removed with a reaction time of 69 min. And the EC was up to 34–227 kWh/kg COD. Obviously, the performances of anodic oxidation are not so satisfactory on phenolic wastewater treatment due to the high EC [9]. These disadvantages also hinder the extensive application of electrochemical oxidation technology. The degradation effectiveness mainly relies on the nature of the electrodes, as well as reactor construction, electrolysis conditions etc.

Carbon membrane as a novel porous inorganic membrane is usually prepared by pyrolysis of various carbonaceous materials, such as polyimide and derivatives, polyacrylonitrile, phenol formaldehyde, and poly (furfuryl alcohol) [10]. These carbon membranes can be extensively used in gas separation [11], energy storage [12], and water treatment [13] due to controllable pore size, excellent chemical stability, and high conductivity [14]. Recently, an electrocatalytic membrane reactor (ECMR) constituted by TiO_2 loading tubular carbon membrane named TiO_2/carbon electrocatalytic membrane as an anode and a stainless steel mesh as a cathode had been employed to treat phenolic wastewater in our previous work [15]. The results showed that the removal rate of phenol and TOC reached approximately 99.4% and 86.3% after 2 h treatment at 2.0 mM phenolic wastewater by ECMR, respectively. The high efficiency and phenol removal obtained are related to the synergistic effect of the electrochemical oxidation and separation or convention-enhanced diffusion in the reactor. During reactor operation, the excitation of TiO_2 would generate reactive intermediate (such as OH, O_2^-, and H_2O_2), which could indirectly decompose the organic foulants on the membrane surface or in the pores or biodegradable products, and thus a high efficiency and low EC were achieved [16,17]. However, the low mechanic strength and loading density of tubular carbon membrane used would seriously limit its practical applications. Besides, the most important issue to be considered is how to enhance convention-enhanced mass transfer rate during the design of an effective electrochemical reactor [18]. Therefore, a fixed-bed electrochemical reactor (FBER) is one of the alternative approaches. In the fixed-bed reactor, the hydrodynamic parameters, mass transfer, effective interfacial area, etc., are dependent on the structure and physical property of carbon membrane electrode such as the thickness.

The objective of this study is to develop a FBER with nano-TiO_2 loading flat-sheet carbon membrane as anode for phenolic wastewater treatment. The electrochemical properties of carbon membranes with four different thicknesses (4.9, 6.3, 7.2, and 10.3 mm) were investigated. The efficiency, EC, and stability of FBER were also explored.

2. Experimental

2.1. Materials

Coal (Shanxi, China) was employed as main raw material. Flat-sheet carbon membrane was prepared by the method described in the literature [19]. Several types of coals were per-grounded into fine particles with a diameter less than 20 μm, and then mixed with cellulose as binder and water. Finally, the coal mixture was obtained. The resultant dough with four different weights was molded into a plate at 10 MPa for 10 min. The resulted plates were preoxidized in an air flow of 100 mL/min at 200°C for 4 h. After that, the preoxidized plates were transferred to a tubular furnace, and then carbonized for 30 min at 950°C with a ramping rate of 3°C/min under a N_2 flow of 100 mL/min. Finally, flat-sheet carbon membranes with the thickness of 4.9 , 6.3 , 7.2, and 10.3 were obtained. All other reagents were of analytical grade and obtained from Tianjin Kermel Chemical Reagent Co., Ltd., China and used without further purification.

2.2. Preparation of TiO_2/carbon membranes

The preparation of TiO_2/carbon membrane was followed by our previous work [17]. The carbon membranes with the thickness of 4.9, 6.3, 7.2, and 10.3 mm were used as the substrate. Tetrabutyl titanate was used as a precursor of TiO_2 sol–gel. A carbon membrane was first pretreated in 65 wt. % HNO_3 solution for 30 min, cleaned up with pure water, and dried at room temperature. The pretreated membrane was immediately dipped into TiO_2 sol for 30 min, then removed from the sol and dried at room temperature. The TiO_2 coated membranes were sintered at 400°C for 2 h in a tubular furnace in N_2 atmosphere to prepare the TiO_2/carbon membrane. Finally, the TiO_2/carbon membrane was obtained. The average pore size, porosity, and bending strength of TiO_2/carbon membranes were summarized in Table 1.

Thereinto, the average pore size and porosity of TiO_2/carbon membranes was measured by mercury intrusion porosimetry (Auto pore IV9500). Cyclic voltammetry (CV) and electrochemical impedance spectroscopy (EIS) measurements were performed with a ZAHNER Zennium Electrochemical Analyzer. The measurements were conducted in a three-electrode system with the TiO_2/carbon membranes as working electrode, Pt as a counter electrode, a saturated calomel electrode (SCE) as the reference. 500 mmol/L KCl and 1.0 mmol/L $K_3[Fe(CN)_6]$ solutions were used as electrolytes. EIS measurements were performed at open-circuit potentials with an amplitude of ±5 mV in the frequency range from 10 mHz to 1 MHz. All solutions were prepared using deionized water.

2.3. Fixed-bed electrochemical reactor

As shown in Fig. 1, a flat-sheet TiO_2/carbon membrane with an effective area of 4 cm^2 as an anode and stainless steel mesh as a cathode were connected by a programmable DC power supply (Maynuo Electronics M8811) to constitute FBER, which was submerged in the feed. The distance between anode and cathode was 15 mm. A peristaltic pump (Longer Pump BT100) was used to suck the filtrate from the feed tank through the membrane to the permeate tank.

Table 1
Average pore size, porosity, and bending strength of TiO_2/carbon membranes

Thickness (mm)	4.9	6.3	7.2	10.3
Average pore size (μm)	0.47	0.54	0.64	0.72
Porosity (%)	35.6	36.7	37.4	38.0
Bending strength (MPa)	9.8	10.8	12.3	16.4

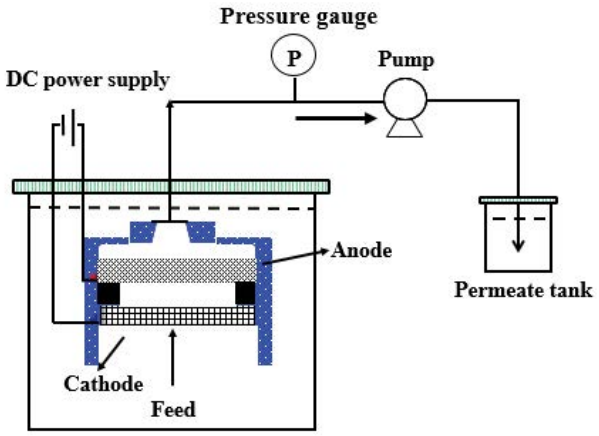

Fig. 1. Schematic diagram of the FBER system.

The degraded permeate can be obtained from the outlet of the peristaltic pump. The FBER was operated under current supply of 0.25–1.25 mA/cm^2. Moreover, the residence time for the phenol inside the membrane can be precisely controlled by adjusting the peristaltic pump speed.

2.4. FBER for phenolic wastewater treatment

The synthetic phenolic wastewater was prepared by mixing 10.0 mmol/L phenol and 15 g/L Na_2SO_4 as the aqueous electrolyte. The phenol concentration was determined by 4-aminoantipyrene spectrophotometric method (UV-Vis Spectrophotometer TU-1901). The phenol removal rate (R_{phenol}) was calculated by the following equation:

$$R_{phenol} = \frac{C_f - C_p}{C_f} \times 100\% \quad (1)$$

where C_f and C_p are the concentration of phenol in the feed (mg/L) and permeate (mg/L), respectively.

The COD of feed and permeate was measured by a COD analyzer (Hach 2800). The removal rate of COD (R_{COD}) was calculated by Eq. (2) as follows:

$$R_{COD} = \frac{COD_f - COD_p}{COD_f} \times 100\% \quad (2)$$

where COD_f and COD_p are the concentration of COD in the feed (mg/L) and permeate (mg/L), respectively.

The EC was calculated by Eq. (3) as follows [20]:

$$EC = \frac{UIt}{3.6(COD_f - COD_p)V} \times 100\% \quad (3)$$

where U is the voltage applied (V), I is the current intensity (A), V is the volume of the permeate (L), and t is the operating time (s).

2.5. The adsorption isotherms of phenol on TiO_2/carbon membrane

Phenol adsorption experiment was carried out with the initial concentration of phenolic wastewater at the range of 1.0–5.0 mmol/L and operating time of 8 h to ensure complete adsorption of TiO_2/carbon membrane with the thickness of 10.3 mm. The permeate flux was kept at 93.8 L/m^2 h. Peristaltic pump provided a driving force and permeate returned back to the feed tank. The amounts of the adsorbed phenol onto TiO_2/carbon membrane (q_e) (mg/g) was calculated by Eq. (4) as follows:

$$q_e = \frac{(C_0 - C_e) \times V}{m} \quad (4)$$

where C_0 is the initial concentration of phenol in the feed (mg/L); C_e is the concentration of phenol in the feed at a certain operating time (mg/L); V is the solution volume (L); and m is the weight of TiO_2/carbon membrane (g).

3. Results and discussions

3.1. The electrochemical properties of TiO_2/carbon membranes

The electrochemical behavior of TiO_2/carbon membranes with four different thicknesses was investigated as shown in Fig. 2. A pair of redox peaks of $Fe^{2+/3+}$ was observed in Fig 2. Further, the peak current (I_p) increased from 1.9 to 7.3 mA with the increase of carbon membrane thicknesses from 4.9 to 10.3 mm. This implied TiO_2/carbon membrane with a thick thickness could effectively increase the electron transfer rate between the membrane electrode surface and $[Fe(CN)_6]^{4-/3-}$. Simultaneously, the higher I_p obtained indicated the membrane electrode with a larger effective surface area because I_p was proportional to the effective surface area [21].

Further, the I_p versus square root of scan rate in the electrolyte solution (1 mmol/L $[Fe(CN)_6]^{4-/3-}$ and 500 mmol/L KCl solution) can be obtained from CVs as demonstrated in Fig. 3. It can be found from Fig. 3 that I_p was linear to $v^{1/2}$ for all four carbon membrane electrodes. According to the Randles–Sevcik equation [22]

$$I_p = 2.69 \times 10^5 n^{3/2} A D^{1/2} v^{1/2} c \quad (5)$$

where n is the number of transfer electron, A is the effective surface area, D is the diffusion coefficient of the electroactive

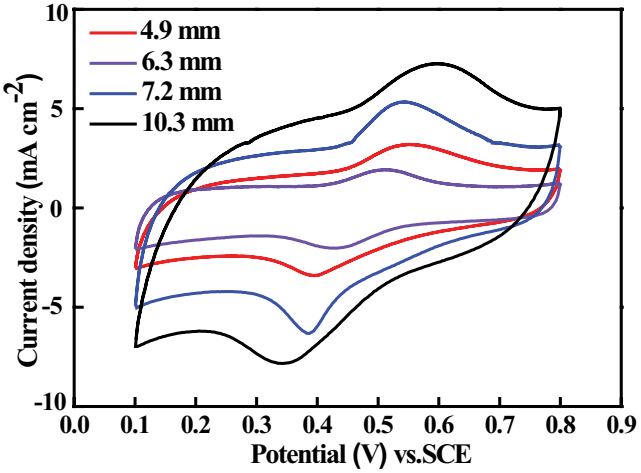

Fig. 2. CVs of TiO_2/carbon membranes with four different thicknesses.

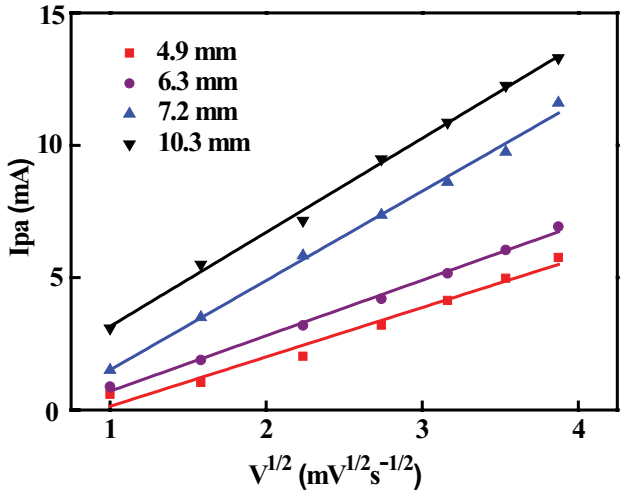

Fig. 3. Peak currents (I_p) versus square root of scan rate during CV measurements of carbon membrane electrodes.

molecule at electrode surface, c is the concentration of the probe molecule, and v is the scan rate.

Herein, for $[Fe(CN)_6]^{4-/3-}$, n = 1, D = 7.6 × 10^{-6} cm^2 /s. The effective surface of the carbon membrane (A) with the thickness of 4.9, 6.3, 7.2, and 10.3 mm obtained from Eq. (5) was 2.83 , 2.95 , 4.55 , and 4.74 cm^2, respectively. Obviously, the thick carbon membrane has a large effective surface area at the same geometric area of 2.0 cm^2.

To further characterize the electrochemical behavior of TiO_2/carbon membranes, that is, a series of electrochemical processes at the interface between the membrane electrode and electrolyte solution, EIS was used to measure the charge transfer resistance (R_{CT}) at the interface between the membrane electrode and electrolytes. EIS measurements were performed in 1.0 mmol/L $[Fe(CN)_6]^{4-/3-}$ containing 500 mmol/L KCl solution at the frequency range from 10 mHz to 1 MHz. The corresponding Nyquist diagram was shown in Fig. 4. The R_{CT} of the reaction was indicated by the diameter of the semicircle at high frequency in the EIS Nyquist plot located within the first quadrant [23,24]. The lower R_{CT} demonstrated the better conductivity of the electrode. According to the simulation of equivalent circuit diagram, R_{CT} obtained from TiO_2/carbon membrane electrodes with the thickness of 4.9 , 6.3 , 7.2 , and 10.3 mm was 4.67 , 4.49 , 2.64 , and 2.49 Ω, respectively. It suggested that TiO_2/carbon membrane with the thickness of 10.3 mm exhibited the greater electron transfer ability in the electro-oxidation, which is in good agreement with the results obtained from CV measurements.

Furthermore, chronoamperometry (CA) was employed to explore electrode reaction processes [22]. The measurements were carried out at the anode potential of 2.5 V. At the same time, a SCE was used as the reference electrode, Pt as the counter electrode, and the carbon membrane as the working electrode. Fig. 5 shows the current intensity versus electrolysis time plot in the CA measurements of the carbon membranes. As shown in Fig. 5, a sharp decline in the current density at the initial time can be observed, and then reached the steady-state. Notably, the steady-state values of current density obtained from carbon membranes with the thickness of 4.9, 6.3, 7.2, and 10.3 mm were 50.0, 53.7, 65.6, and 75.8 mA/cm^2, respectively. It implied that a thick carbon membrane is advantageous for the reactant molecules to be moved to the surface of the electrode so as to lead to a reduction in the thickness of diffusion layer and more $[Fe(CN)_6]^{4-/3-}$ to be transferred to the surface of the electrode, finally resulting in an increase at the reaction rate [25].

In addition, as an important parameter of reaction kinetics, diffusion coefficient (D) reflects the characteristics of diffusion and mass transfer of the electrochemical system. The diffusion coefficient of reaction kinetics during the electrochemical reaction also can be obtained from CA measurements. At first, the curve of I_p versus $t^{-1/2}$ obtained from the carbon membranes is illustrated in Fig. 6. Then the diffusion coefficient can be obtained from the slope of the linear fitting curve in Fig. 6 according to the combination Cottrell's equation [26].

$$i = nFAD^{1/2}c_b^{-1/2}t^{-1/2} \quad (6)$$

where D is the apparent diffusion coefficient (cm^2 /s), c_b is the bulk concentration (mol/cm^3) of $[Fe(CN)_6]^{4-/3-}$, F is Faraday

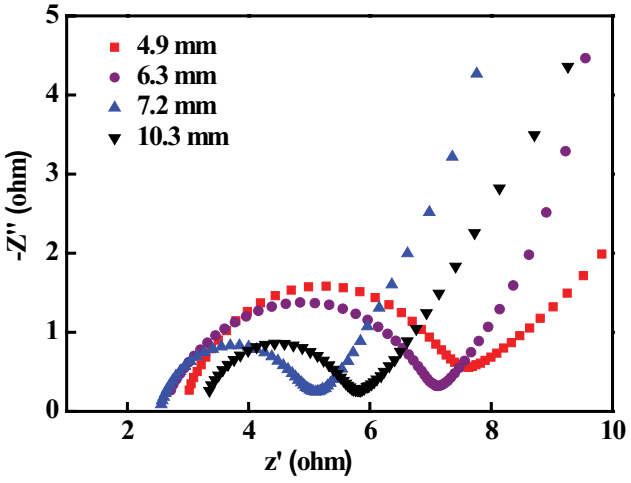

Fig. 4. EIS Nyquist plots of TiO_2/carbon membrane electrodes with four different thicknesses.

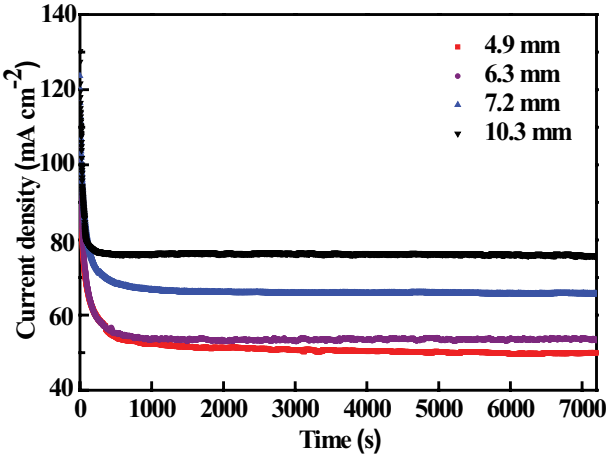

Fig. 5. Chronoamperometry for the carbon membranes with four thickness.

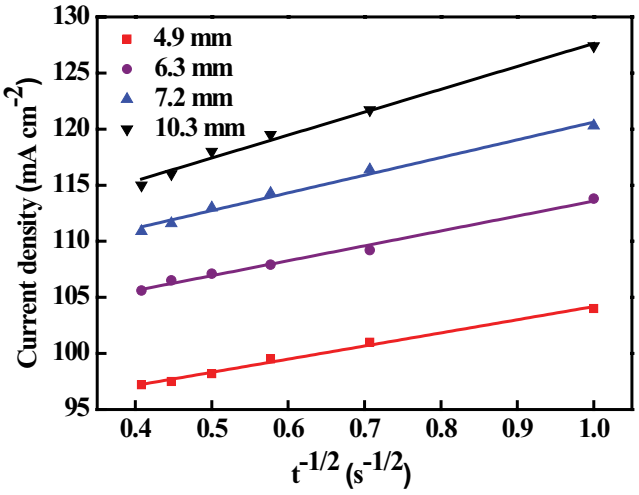

Fig. 6. The curve of I_p versus $t^{-1/2}$ for the carbon membranes with four thicknesses.

constant, A is the effective surface area, and n is the electron transfer number of $[Fe(CN)_6]^{4-/3-}$.

Finally, the fitting slopes of I–$t^{-1/2}$ and diffusion coefficients obtained from carbon membranes with four different thicknesses are shown in Table 2. It can be seen from Table 2 that the carbon membrane with the thickness of 10.3 mm had a largest diffusion coefficient (6.88×10^{-3} cm^2/s). In short, the lower mass transfer resistance and higher electron transfer ability of carbon membranes with the thickness of 10.3 mm scavenging additional ferrocyanide at the electrode interface leading to a largest diffusion coefficient [27].

3.2. The performance of FBER

In order to further investigate the catalytic properties, the TiO_2/carbon membrane was employed as an anode to constitute FBER for the treatment of 10.0 mmol/L phenol wastewater under the operating conditions of the current density of 1.0 mA/cm^2 and reaction time of 7.8 min. At the same time, 15 g/L Na_2SO_4 was used as an electrolyte. The phenol and COD removal rate are demonstrated in Fig. 7. It can be seen from Fig. 7 that the phenol and COD removal rates obtained from FBER increased from 89.3% to 97.5% with the increase of carbon membrane electrode thickness from 4.9 to 10.3 mm. In particular, the EC declined from 0.88 to 0.36 kWh/kg COD with the increase of carbon membrane electrodes from 4.9 to 10.3 mm as shown in Fig. 7. It suggested that the carbon membrane electrode with the thickness of 10.3 mm presented excellent catalytic oxidation performance and a low EC. Certainly, the thickness of carbon membrane electrode is also closely related to its hydrodynamic resistance and the permeability in the practical applications.

Table 2
Linear fitting slopes of I–$t^{-1/2}$ and diffusion coefficients

Thickness (mm)	4.9	6.3	7.2	10.3
Fits slope of I vs. $t^{-1/2}$	11.72	13.29	15.77	20.42
D (10^{-3} cm^2/s)	3.45	4.47	5.31	6.88

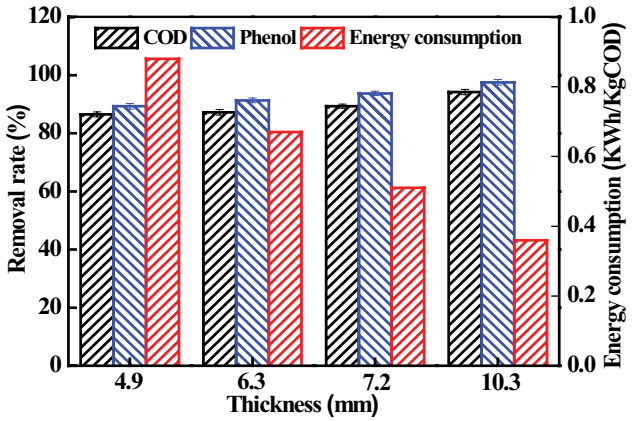

Fig. 7. COD, phenol removal rate, and energy consumption of FBER with different thicknesses of carbon membrane electrodes.

Herein, the membrane hydraulic resistance (R_m) and permeability coefficient can be obtained from the permeate flux according to Darcy's law as follows [28]:

$$J = \frac{\Delta P}{\mu R_m} \tag{7}$$

where J is the pure water permeate flux (L/m^2/h/bar), ΔP is the transmembrane pressure (Pa), μ is the viscosity of water (0.894 mPa s at 25°C), and R_m is hydraulic resistance (m^{-1}).

According to Eq. (7), hydraulic resistance and permeability coefficient can be calculated as shown in Fig 8. It can be found from Fig. 8 that the membrane resistance increased from 0.621×10^{12} to 1.79×10^{12} m^{-1} with an increase in the thickness of carbon membrane from 4.9 to 10.3 mm. On the contrary, the permeability coefficient declined from 648 to 225 L/m^2/h/bar. Obviously, the increase of carbon membrane thickness would lead to the increase of hydrodynamic resistance and the decline of permeability coefficient, leading to a high kinetic energy cost under the same permeate flux. Therefore, the selection of a proper thickness membrane needs to consider the balance between kinetic energy and catalytic efficiency of the reactor.

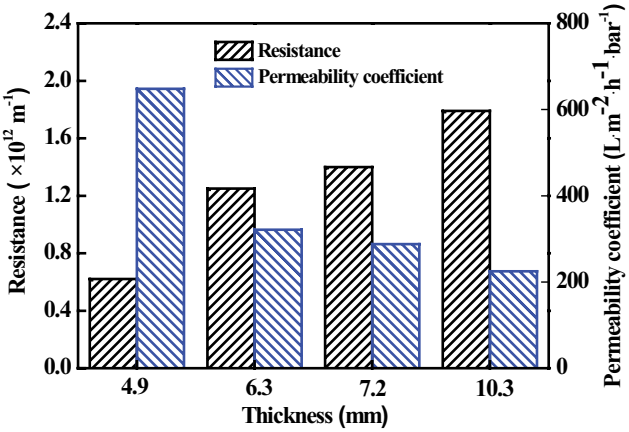

Fig. 8. Hydraulic resistance and permeability coefficient of carbon membranes.

3.3. Adsorption isotherms of phenol on TiO_2/carbon membrane

According to the mechanism of electrochemical oxidation, the diffusion of organic chemicals from the feed solution to the electrode surface is the key step during electro-oxidation processes [29]. And that the improvement of adsorption ability is favor of the diffusivity coefficient enhancement [1]. TiO_2/carbon membrane with specific chemical and porous structure is beneficial for phenol adsorption. The adsorption isotherms of phenol on TiO_2/carbon membrane at room temperature is illustrated in Fig. 9. It can be seen from Fig. 9 that the amount of adsorbed phenol increased from 0.13 to 0.43 mg/g with the increase of equilibrium concentration from 85 to 440 mg/L.

According to the adsorption isotherms of phenol on TiO_2/carbon membrane, the Langmuir and Freundlich models can be used to analyze the adsorption kinetics. The Langmuir equation is described as Eq. (8) [30]:

$$q_e = \frac{Q_0 K_L C_e}{1 + K_L C_e} \tag{8}$$

where Q_0 (mg/g) is the Langmuir constants, representing the maximum adsorption capacity for the solid-phase loading; K_L (L/mg) is the energy constant related to the heat of adsorption [31]. The Freundlich equation is described as Eq. (9) [30]:

$$q_e = K_F C_e^{\frac{1}{n}} \tag{9}$$

where K_F ($mg^{1-1/n}\ L^{1/n}\ g$) is the Freundlich constants and n is the fitted parameters using two models as listed in Table 3.

The coefficient (R^2) is used as a measure of goodness of fit of model. It can be seen from Table 3 that the value of R^2 obtained from Langmuir and Freundlich models was 0.9934 and 0.9962, respectively. It indicated that the fitted Langmuir and Freundlich models could explain 99.3% and 99.6% of variability, respectively. The accuracy and general ability of the polynomial model was reliable. It also suggested that the phenol adsorption on TiO_2/carbon membrane was a physical adsorption [32]. The maximum adsorption capacity obtained by Langmuir model was 1.06 mg/g. The adsorption of phenol molecules toward the anode surface has a significant effect on the electrochemical oxidation processes [29].

Table 3
Fitted parameters of Langmuir and Freundlich models for phenol adsorption on TiO_2/carbon membrane

Langmuir			Freundlich		
Q_0(mg/g)	K_L(L/mg)	R^2	K_F ($mg^{1-1/n}\ L^{1/n}\ g$)	1/n	R^2
1.06	1.67×10^{-3}	0.9934	5.32×10^{-3}	0.725	0.9962

3.4. FBER stability

As mentioned in Section 2, an FBER constituted by TiO_2/carbon membrane with the thickness of 10.3 mm as anode and a stainless steel mesh as cathode had been employed to treat phenolic wastewater. An FBER stability experiment of 12 h for 10.0 mmol/L phenolic wastewater was carried out under the following conditions: residence time of 7.8 min and current density of 1.0 mA/cm^2. The phenol and COD removal rate obtained from FBER versus operating time are illustrated in Fig. 10. It can be observed from Fig. 10 that the removal rate of phenol (97% ± 0.5%) and COD (89% ± 0.5%) kept stable at 12 h of the operating. It suggested that the carbon membrane and FBER exhibited a high efficiency and stability.

3.5. The removal mechanism of phenol on FBER

During the FBER operation, the TiO_2 on the membrane was electrified to generate the electron/hole pair, which interacted with H_2O to produce hydroxyl radicals on the membrane surface [16,17]. The hydroxyl radicals generated in the FBER were apt to electrophilically attack the adjacent or *para*-position of phenol to produce hydroquinone and catechol, which as the main intermediates were easily further oxidized to *p*-benzoquinone. Under further oxidation by the hydroxyl radicals, the conjugate structure of the benzene ring from *p*-benzoquinone would be disconnected and produced maleic acid, oxalic acid, and other small molecules acid [15]. Further, when the hydroxyl free radicals were sufficient, phenol and produced intermediates would be completely mineralized into CO_2 and H_2O [33].

4. Conclusions

Nano-TiO_2 loading flat-sheet microporous carbon membranes were successfully prepared and employed to

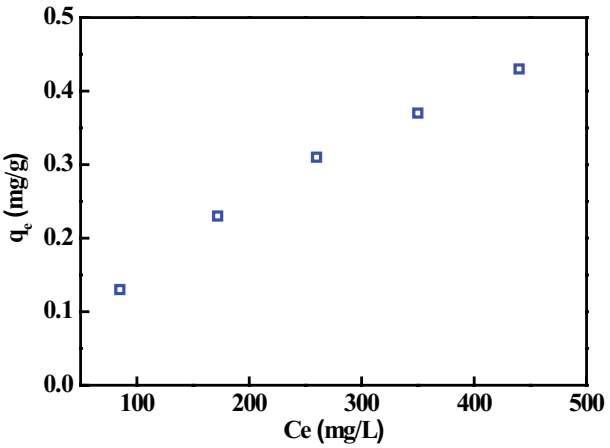

Fig. 9. Adsorption isotherms of phenol on TiO_2/carbon membrane.

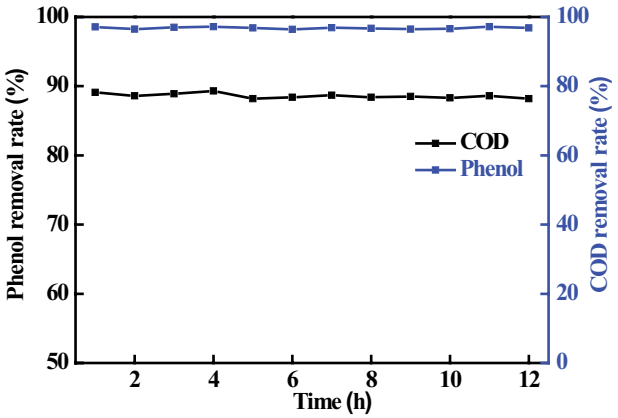

Fig. 10. Removal rate of phenol and COD during the FBER operating.

constitute FBER for phenolic wastewater treatment. The TiO_2/carbon membrane with a thicker thickness exhibited an excellent electrochemical performance owing to a large effective surface area and the great electron transfer ability. It is noted that the thickness of carbon membrane electrode is also closely related to its hydrodynamic resistance and the permeability. Further, the removal rates of phenol and COD obtained by FBER with the thickness of 10.3 mm under the operating conditions of 10.0 mmol/L phenolic wastewater, residence time of 7.8 min, and current density of 1.0 mA/cm^2 were up to 89.3% and 97.5%, respectively. The adsorption of phenol molecules toward the anode surface played a key role on the electrochemical oxidation processes. The maximum adsorption capacity obtained by Langmuir model was 1.06 mg/g. Furthermore, the EC of FBER was only 0.36 kWh/kg COD. FBER also exhibited an excellent stability.

Acknowledgments

We gratefully acknowledge the financial supports for this work from National Natural Science Foundation of China (Grant no. 21576208, 21676200, and 51608361), the Chang-jiang Scholars, and Innovative Research Team in the University of Ministry of Education, China (Grant no. IRT-17R80).

References

[1] M.A. Ajeel, M.K. Aroua, W.M.A.W. Daud, S.A. Mazari, Effect of adsorption and passivation phenomena on the electrochemical oxidation of phenol and 2-Chlorophenol at carbon black diamond composite electrode, Ind. Eng. Chem. Res., 56 (2017) 1652–1660.
[2] W. Kujawski, A. Warszawski, W. Ratajczak, Removal of phenol from wastewater by different separation techniques, Desalination, 163 (2004) 287–296.
[3] J. Chen, L. Zhang, Q. Jin, C.Z. Su, L. Zhao, X.X. Liu, S.M. Kou, Y.J. Wang, M. Xiao, Bioremediation of phenol in soil through using a mobile plant-endophyte system, Chemosphere, 182 (2017) 194–202.
[4] M. Pérez, F. Torrades, Removal of organic contaminants in paper pulp treatment effluents under Fenton and photo-Fenton conditions, Appl. Catal., B, 36 (2002) 63–74.
[5] A.M. Amat, A. Arques, F. López, M.A. Miranda, Solar photocatalysis to remove paper mill wastewater pollutants, Solar Energy, 79 (2005) 393–401.
[6] O. Abdelwahaba, N.K. Amin, E.-S.Z. El-Ashtoukhy, Electrochemical removal of phenol from oil refinery wastewater, J. Hazard. Mater., 163 (2009) 711–716.
[7] X.P. Zhu, J.R. Ni, J.J. Wei, X.A. Xing, H.N. Li, Y. Jiang, Scale-up of B-doped diamond anode system for electrochemical oxidation of phenol simulated wastewater in batch mode, J. Hazard. Mater., 184 (2010) 493–498.
[8] J.J. Wei, X.P. Zhu, J.R. Ni, Electrochemical oxidation of phenol at boron-doped diamond electrode in pulse current mode, Electrochim. Acta, 56 (2011) 5310–5315.
[9] E. Fockedey, A.V. Lierde, Coupling of anodic and cathodic reactions for phenol electro-oxidation using three-dimensional electrodes, Water Res., 36 (2002) 4169–4175.
[10] A.F. Ismail, L.I.B. David, A review on the latest development of carbon membranes for gas separation, J. Membr. Sci., 193 (2001) 1–18.
[11] Y.J. Fu, C.C. Hu, D.W. Lin, H.A. Tsai, S.H. Huang, W.S. Hung, K.R. Lee, J.Y. Lai, Adjustable microstructure carbon molecular sieve membranes derived from thermally stable polyetherimide/polyimide blends for gas separation, Carbon, 113 (2017) 10–17.
[12] F. Ran, K.W. Shen, Y.T. Tan, B.W. Peng, S.H. Chen, W.J. Zhang, X.Q. Niu, L.B. Kong, L. Kang, Activated hierarchical porous carbon as electrode membrane accommodated with triblock copolymer for supercapacitors, J. Membr. Sci., 514 (2016) 366–375.
[13] X.P. Chen, H. Wang, Y. Yang, B.Q. He, J.X. Li, T.H. Wang, The surface modification of coal-based carbon membranes by different acids, Desal. Wat. Treat., 51 (2013) 5855–5862.
[14] G.T. Qin, X.F. Cao, H. Wen, W. Wei, C. João, D. Costa, Fine ultramicropore control using the intrinsic viscosity of precursors for high performance carbon molecular sieve membranes, Sep. Purif. Technol., 177 (2017) 129–134.
[15] H. Wang, Q.Q. Guan, J.X. Li, T.H. Wang, Phenolic wastewater treatment by an electrocatalytic membrane reactor, Catal. Today, 6 (2014) 121–126.
[16] Y. Yang, J.X. Li, H. Wang, X.K. Song, T.W. Wang, B.Q. He, X.P. Liang, H.H. Ngo, An electrocatalytic membrane reactor with self-cleaning function for industrial wastewater treatment, Angew. Chem. Int. Ed., 50 (2011) 2148–2150.
[17] Y. Yang, H. Wang, J.X. Li, B.Q. He, T.H. Wang, S. Liao, Novel functionalized nano-TiO_2 loading electrocatalytic membrane for oily wastewater treatment, Environ. Sci. Technol., 46 (2012) 6815–6821.
[18] Y.F. Ling, H.L. Xu, X.M. Chen, Continuous multi-cell electrochemical reactor for pollutant oxidation, Chem. Eng. Sci., 122 (2015) 630–636.
[19] C. Wang, F. Meng, T.H. Wang, T.L. Ma, J.S. Qiu, Monolithic coal-based carbon counter electrodes for highly efficient dye-sensitized solar cells, Carbon, 67 (2014) 465–474.
[20] B. Wang, W. Kong, H. Ma, Electrochemical treatment of paper mill wastewater using three-dimensional electrodes with Ti/Co/SnO_2-Sb_2O_5 anode, J. Hazard. Mater., 146 (2007) 295–301.
[21] C.H. Lee, E.S. Lee, Y.K. Lim, K.H. Park, H.D. Park, D.S. Lim, Enhanced electrochemical oxidation of phenol by boron-doped diamond nanowire electrode, RSC Adv., 7 (2017) 6229–6235.
[22] Y. Huang, H.J. Yan, Y.J. Tong, Electrocatalytic determination of reduced glutathione using rutin as a mediator at acetylene black spiked carbon paste electrode, J. Electroanal. Chem., 743 (2015) 25–30.
[23] J. Yoshida, K. Kataoka, R. Horcajada, A. Nagaki, Modern strategies in electroorganic synthesis, Chem. Rev., 108 (2008) 2265–2299.
[24] B.A. Frontana-Uribe, R.D. Little, J.G. Ibanez, A. Palma, R. Vasquez-Medrano, Organic electrosynthesis: a promising green methodology in organic chemistry, Green Chem., 12 (2010) 2099–2119.
[25] E.S. Takeuchi, R.W. Murray, Metalloporphyrin containing carbon paste electrodes, J. Electroanal. Chem. Interfacial Electrochem., 189 (1985) 49–57.
[26] J.H. Li, J. Li, H.B. Feng, Y.Q. Zhang, J.B. Jiang, Y.L. Feng, M.S. Chen, D. Qian, A facile one-step in situ synthesis of copper nanostructures/graphene oxide as an efficient electrocatalyst for 2-naphthol sensing application, Electrochim. Acta, 153 (2015) 352–360.
[27] K.N. Kuo, R.W. Murray, Electrocatalysis with ferrocyanide electrostatically trapped in an alkylaminesiloxane polymer film on a Pt electrode, J. Electroanal. Chem. Interfacial Electrochem., 131 (1982) 37–59.
[28] M.C.V. Vela, S.Á. Blanco, J.L. García, E.B. Rodríguez, Application of a dynamic model for predicting flux decline in crossflow ultrafiltration, Desalination, 198 (2006) 303–309.
[29] Y.Y. Chu, W.J. Wang, M. Wang, Anodic oxidation process for the degradation of 2, 4-dichlorophenol in aqueous solution and the enhancement of biodegradability, J. Hazard. Mater., 180 (2010) 247–252.
[30] S.H. Lin, R.S. Juang, Adsorption of phenol and its derivatives from water using synthetic resins and low-cost natural adsorbents: a review, J. Environ. Manage., 90 (2009) 1336–1349.
[31] K. Mohanty, D. Das, M.N. Biswas, Adsorption of phenol from aqueous solutions using activated carbons prepared from tectona grandis sawdust by $ZnCl_2$ activation, Chem. Eng. J., 115 (2005) 121–131.
[32] Q. Liao, J. Sun, L. Gao, The adsorption of resorcinol from water using multi-walled carbon nanotubes, Colloids Surf., A, 312 (2008) 160–165.
[33] Y.J. Shen, L.C. Lei, X.W. Zhang, M.G. Zhou, Y. Zhang, Effect of various gases and chemical catalysts on phenol degradation pathways by pulsed electrical discharges, J. Hazard. Mater., 150 (2008) 713–722.